Crystallization Behavior of Nylon 11/Montmorillonite Nanocomposites Under Annealing

Xikui Zhang,[1] Guisheng Yang,[2] Jiaping Lin[1]

[1]*Material Science and Engineering Institute, East China University of Science and Technology, Shanghai 200237, People's Republic of China*
[2]*Key Laboratory of Engineering Plastics, Joint Laboratory of Polymer Science and Materials, Institute of Chemistry, Chinese Academy of Sciences, Beijing 100080, People's Republic of China*

Received 5 September 2005; accepted 18 November 2005
DOI 10.1002/app.23900
Published online in Wiley InterScience (www.interscience.wiley.com).

ABSTRACT: Exfoliated nylon 11/montmorillonite (MMT) nanocomposites were prepared via *in situ* polymerization by the dispersion of organically modified MMT in 11-aminoundecanoic acid monomer. The polymorphic behavior of the nylon 11/MMT nanocomposites was investigated with X-ray diffraction, transmission electron microscopy, and Fourier transform infrared with attenuated total reflectance. MMT induced and stabilized the δ-crystalline form of nylon 11. The crystal structure of nylon 11 was transformed from a hexagonal δ-form structure to a triclinic α-form structure during the annealing process. Meanwhile, the hydrogen bonds in the nanocomposites also exhibited some differences from neat nylon 11 after annealing. © 2006 Wiley Periodicals, Inc. J Appl Polym Sci 102: 5483–5489, 2006

Key words: crystallization; nanocomposites; nylon

INTRODUCTION

Applications of layered silicate as fillers in polymers have received considerable attention in recent years. It has been demonstrated that a high-aspect-ratio layered-silicate leads to dramatic enhancements in the properties in comparison with conventional microcomposites.[1–3] The impressive mechanical properties of polymer/clay nanocomposites, that is, nylon 6/clay nanocomposites,[4–6] were first demonstrated by a group at the Toyota research center in Japan. Since then, many polymer/clay nanocomposite systems have been prepared and investigated. The effect of clay on the crystal structure of the matrix is of interest. Early investigations of the nylon 6 matrix suggested that the γ-crystalline form was enhanced by the addition of the clay.[7–10] Although the property enhancements of polymer/clay nanocomposites can be explained by the exfoliation and dispersion of montmorillonite (MMT) layers in a matrix, some property changes may be related to the crystalline modification of the polymer matrix.[10–13]

The residual stress formed during the preparation of polymer/clay nanocomposites could affect the microstructure and properties of the composites. Thermal annealing can be used to remove residual stress during processing thereafter and has been shown to change the crystalline structure in polyimide and polyamide.[14,15] Gurato et al.[16] and Gogolewski et al.[17] demonstrated the conversion of the crystal structure of nylon 6/clay nanocomposites by an annealing treatment. A similar phenomenon was also observed in nylon 66/clay nanocomposites.[18]

Nylon 11 is a semicrystalline polymer and exhibits at least five crystalline forms, including the α form resulting from the annealing of a quenched sample or solution casting from *m*-cresol, the α′ form obtained from melt crystallization, the δ form corresponding to a high-temperature α form, the δ′ form obtained via melt quenching, and the γ form obtained via solution casting from trifluoroacetic acid.[19–26] The α and α′ forms have a triclinic structure, but the other three forms have a hexagonal or pseudohexagonal structure.

By now, research is mainly focused on the influence of clay on the crystallization of nylon 11.[27,28] As nylon 6/clay hybrid materials exhibit excellent properties, it is expected that the properties of nylon 11 will also be improved by the preparation of its corresponding nanocomposites. However, the effects of layered MMT on the crystallization of nylon 11 have received little attention, especially the influence of annealing treatments.

In general, the gallery distance of clay should play an important role in determining the degree of exfoliation of clay aggregates. Therefore, it is very important to match the chemical affinity between the polymer matrix and clay. In this study, we modified the original clay with 11-aminoundecanoic acid by a novel method.

Correspondence to: X. Zhang (xikuizhang@163.com).
Contract grant sponsor: National 973 Project; contract grant number: 2003CB615602.
Contract grant sponsor: Shanghai Genius Advanced Materials Co., Ltd.

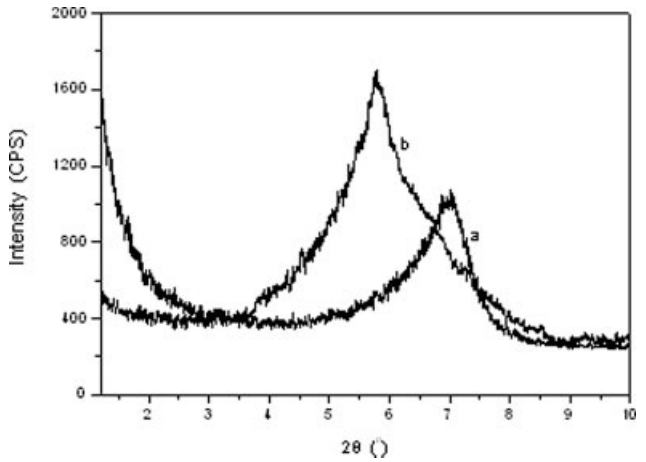

Figure 1 XRD patterns of (a) the original clay and (b) the organoclay.

Thus, the layered clay could be compatible with the nylon 11 matrix and could achieve exfoliation. In this work, a series of nylon 11 nanocomposites with different degrees of clay intercalation and exfoliation were prepared via *in situ* polymerization. The nanocomposites were characterized with X-ray diffraction (XRD), transmission electron microscopy (TEM), and Fourier transform infrared (FTIR) with attenuated total reflectance. We clarified the possibility of the δ′ and δ phases with the presence of MMT and investigated the effects of MMT on the crystallization behavior of nylon 11. The crystalline-structure changes of nylon 11/MMT nanocomposites under thermal annealing were also characterized and examined.

EXPERIMENTAL

Material preparation

The monomer, 11-aminoundecanoic acid, was commercially available. The pristine silicate clay was supplied by Zhejiang Fenghong Clay Chemicals Co., Ltd. (China). The cation-exchange capacity of the Na–MMT used in this study was 80 mequiv/100 g, and the water content was about 7 wt % in the original state (thermogravimetric analysis method). Organically modified MMT was prepared as follows. MMT (100 g) was dispersed into 5000 mL of hot water with a homogenizer. 11-Aminoundecanoic acid (8.0 g) and 4 mL of concentrated hydrochloric acid were dissolved in hot water (200 mL) and then poured into the MMT water suspension with vigorous stirring for 12 h. The product was filtered off, washed three times, and dried in a vacuum oven.

A wide range of nylon 11/organoclay nanocomposites containing 1, 2, 4, or 6 wt % organoclay was prepared via *in situ* polymerization. First, 11-aminoundecanoic acid was mixed with the organoclay in a vessel, and then the mixtures were heated at 100–150°C to drive off the water and heated again at 230–260°C for 4 h to achieve polymerization. The neat nylon 11 was prepared with the same procedure. The samples were annealed at 160°C for different times in the range of 0–24 h and then gradually cooled to room temperature.

The neat nylon 11 and the nanocomposite pellets were placed in a mold that was positioned between two steel plates covered with aluminum foil. Film samples (0.1 mm thick) were prepared via compression molding in a press at a temperature of 220°C and a pressure of 150 bar, followed by quick quenching in an ice–water bath to obtain amorphous sheets.

Measurements

The XRD measurements were performed at room temperature with a Rigaku D/max 2550 diffractometer operating at a voltage of 40 kV and a current of 100 mA with a curved graphite crystal filtered with Cu Kα radiation ($\lambda = 0.154056$ nm). The scanning rate was 4°/min, and the scanning ranges were 1.2–10 and 3–50°. The data were collected at step intervals of 0.02°.

The TEM measurements of the nanocomposite specimens without staining were taken at room temperature with a Hitachi H-600 transmission electron microscope operated at 120 kV. The ultrathin films (50–70 nm thick) were performed at −60°C for nylon 11/organically modified MMT nanocomposites with a Leica Ultracut-E microtome with a diamond knife.

IR spectra were collected at a resolution of 4 cm^{-1} with a Nicolet Avatar 360 FTIR spectrometer in its attenuated total reflectance mode.

RESULTS AND DISCUSSION

Nanostructure and morphology

Figure 1 shows the XRD patterns of pristine silicate clay and organoclay modified with 11-aminoundeca-

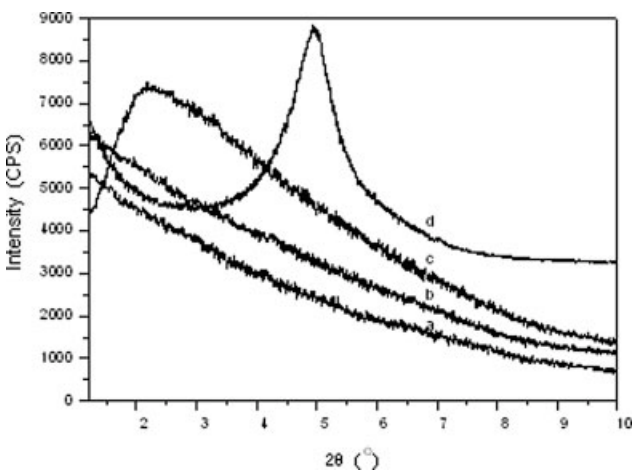

Figure 2 XRD patterns of nylon 11/MMT nanocomposites with different MMT concentrations: (a) 1, (b) 2, (c) 4, and (d) 6 wt %.

noic acid. The characteristic diffraction peaks corresponded to the (001) reflections plane of MMT. The XRD pattern of the pristine clay mineral showed a reflection peak at about $2\theta = 7.1^\circ$, corresponding to a basal spacing of 1.38 nm. For the organoclay, the reflection peak of the basal plane dramatically shifted to $2\theta = 5.8^\circ$ with a *d*-spacing of 1.53 nm. The obviously increased layer distance demonstrated that 11-aminolauric acid diffused into the clay galleries to increase the layer distance, and a swollen and intercalated structure was formed in the organoclay.

The dispersion of the MMT layers in the nylon 11 matrix was evidenced by XRD, as shown in Figure 2. The reflection peak of the (001) crystal plane shifted to $2\theta = 5.0^\circ$ [Fig. 2(d)] and $2\theta = 2.2^\circ$ [Fig. 2(c)], thus corresponding to the basal spacings of 1.76 and 3.47 nm, respectively. This suggested that the nylon 11 molecules entered the interlayer spacing and increased the *d*-spacing. However, in Figure 2(a,b), there was no characteristic peak corresponding to the MMT basal spacing. The absence of basal plane peaks indicated that the homogeneous and exfoliated nanocomposite structures existed within the nylon 11 matrix when the MMT concentration was less than 4 wt %. As the MMT concentration increased up to a critical value, the aggregation of silicate layers in the matrix occurred, and the intensity of the (001) characteristic diffraction peaks increased.

Figure 3 presents TEM images of nylon 11/organoclay nanocomposites; the dark areas represent the clay, and the gray/white areas represent the polymer matrix. Each layer of clay was disordered and dispersed homogeneously in nylon 11. This was consistent with the absence of the (001) plane peak in Figure 2 due to

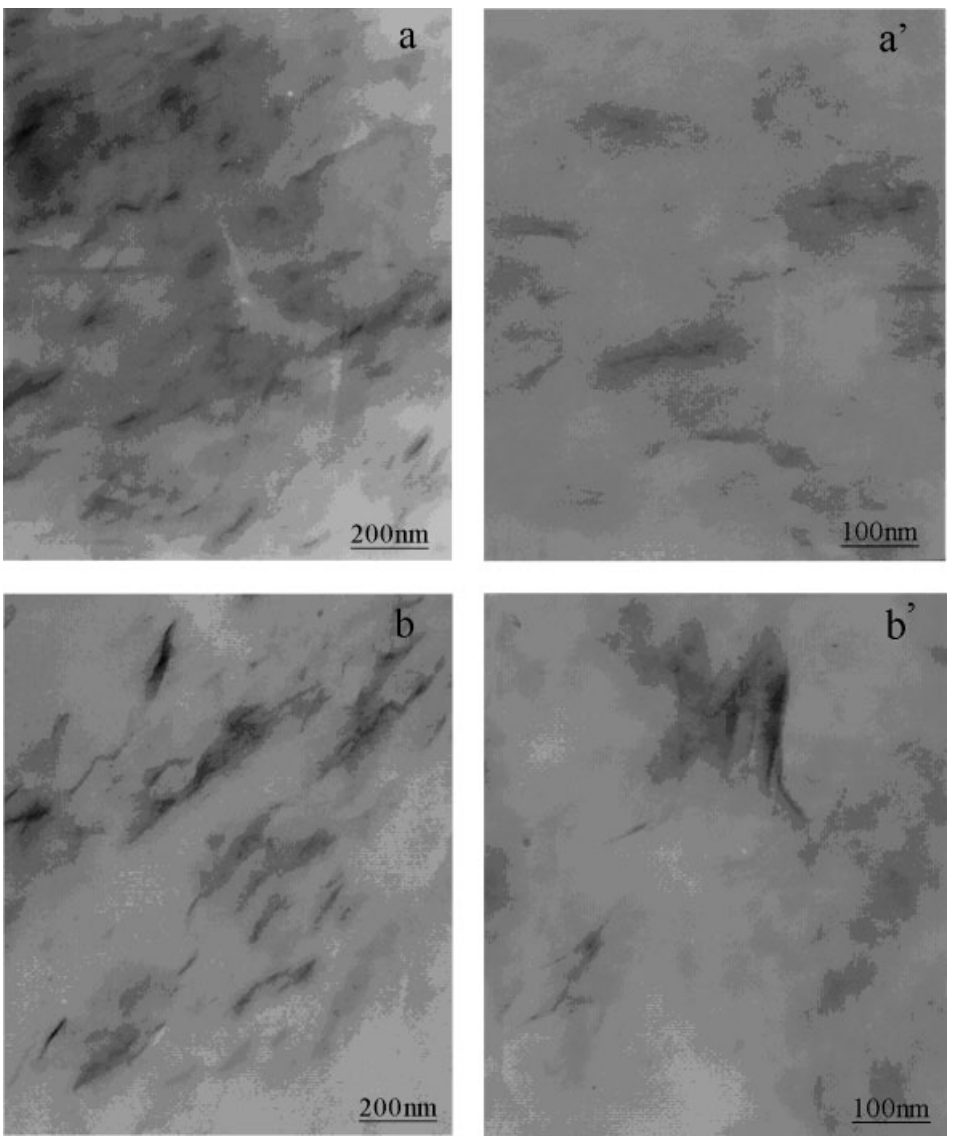

Figure 3 TEM images of nylon 11/MMT nanocomposites: (a) 2 wt % MMT and (b) 6 wt % MMT. Images a′ and b′ are local magnifications of images a and b, respectively.

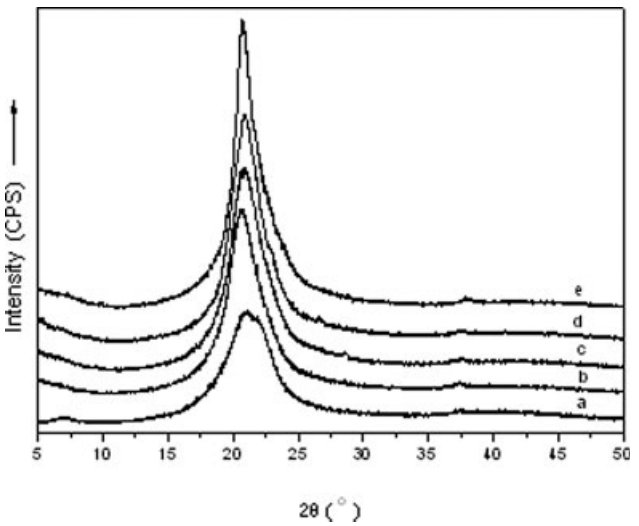

Figure 4 WAXD patterns of nylon 11/MMT nanocomposites with different MMT concentrations: (a) 0, (b) 1, (c) 2, (d) 4, and (e) 6 wt %.

the very large interlayer spacing and the disordered state of the clay layer. Figure 3 shows that the clay dispersed in the nylon 11 matrix well, and the degree of dispersion of the clay aggregates in sample NC-2 was much higher than that of sample NC-6. Clearly, the former (with a low clay loading of 2 wt %) was typical of a disordered and exfoliated clay nanostructure, whereas the latter (with a high clay loading of 6 wt %) had a typically ordered intercalated nanoclay morphology. This observation was also consistent with that made from the XRD patterns given in Figure 2.

Figure 4 displays the wide-angle X-ray diffraction (WAXD) patterns of nylon 11/MMT nanocomposites with different concentrations of MMT. Figure 4(a) shows one strong and broad reflection (100) with a *d*-spacing of 0.42 nm, which was characteristic of the δ′ form of nylon 11. This crystal structure was determined to be a smectic phase.[29] The other WAXD patterns [Fig. 4(b–e)] show a stronger and sharper reflection at about 0.43 nm with increasing MMT concentration than that of Figure 4(a); these changes demonstrate the characteristic δ form produced from the δ′ form.[20] It is suggested that the addition of silicate layers forced the amide groups of nylon out of the hydrogen-bond sheet, resulting in the conformational change of the molecular chains and restricting the formation of hydrogen-bond sheets.[30] The addition of MMT forced the amide groups of nylon 11 out of the extended sheet, resulted in the tilting of the amide group and the formation of the δ phase. This trend also indicated that the degree of crystallinity of the hexagonal δ form increased with an increase in the MMT concentration; that is, the higher the MMT concentration was, the more perfect the crystallization of nylon 11 was.

Influence of annealing on the crystalline structure

Figure 5 presents the WAXD patterns of nylon 11 annealed at 160°C for different times. The original sample [Fig. 5(a)] exhibited only one strong and broad reflection (100) at $2\theta = 21.5^\circ$ with a *d*-spacing of 0.42 nm, which was characteristic of the pseudohexagonal δ′ form. When the sample was annealed at 160°C, the (100) reflection split into two reflections, and these two reflections split more obviously with increasing annealing time. The annealing treatment increased the reflection intensity, and the separation of the two reflections became more obvious, thus leading to the crystal transformation from the pseudohexagonal δ′ form to the triclinic α form. The thermal treatment favored the formation of the α form rather than the δ′ form in nylon 11, as the α form was the thermodynamically more stable crystalline form. These results also indicated that the prolonged annealing time of nylon 11 improved the crystal perfection of the polymer.[31]

Figure 6 shows the WAXD patterns of the nylon 11/MMT nanocomposites with various MMT contents annealed at 160°C for different times. The original sample [Fig. 6(a)] exhibited only one strong reflection (100), which was characteristic of the δ form. When the composites were annealed at 160°C for different times, the (100) reflection of the δ form split into two reflections, and these two reflections split more obviously with increasing annealing time [Fig. 6(b–g)]. The two reflections were indexed as (100) and (010,110) planes because the nylon 11/MMT nanocomposites crystallized in the triclinic α-form structure. These two reflections corresponded to the distance between hydrogen-bonded chains in sheets and the separation of the hydrogen-bond sheets, respectively.[32]

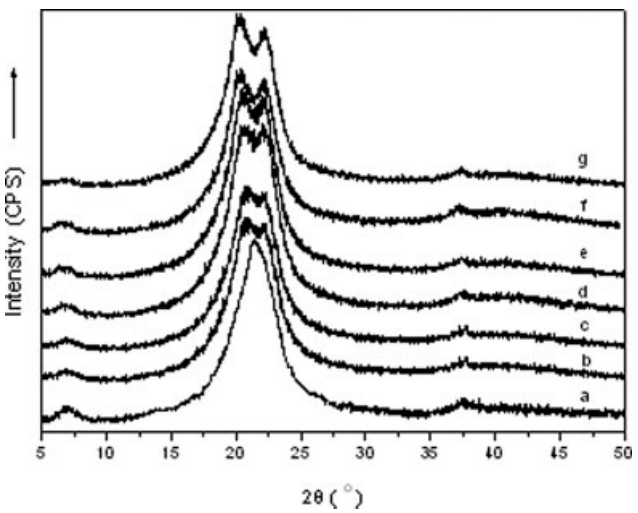

Figure 5 WAXD patterns of nylon 11 annealed at 160°C for different times: (a) 0, (b) 0.25, (c) 1, (d) 3, (e) 6, (f) 12, and (g) 24 h.

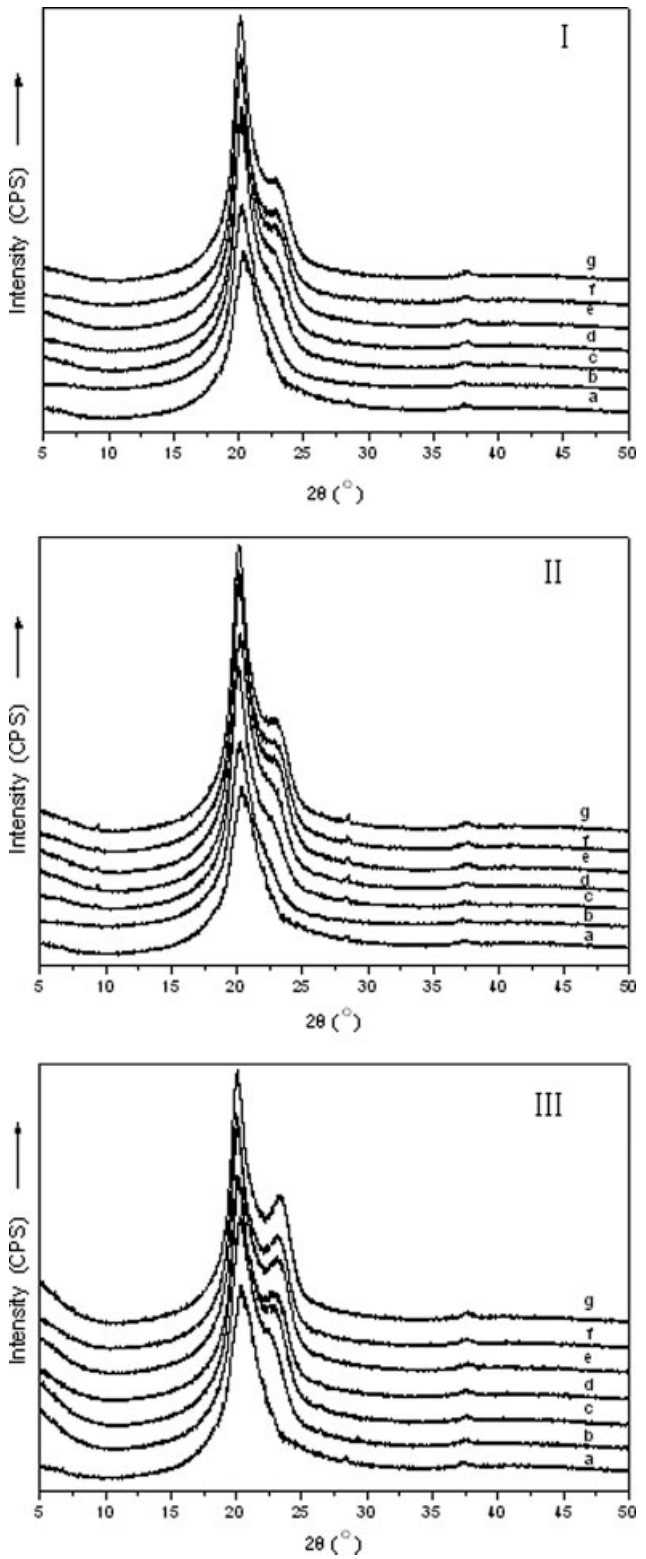

Figure 6 XRD patterns of nylon 11/MMT nanocomposites with (I) 1, (II) 2, or (III) 4 wt % MMT annealed at 160°C for different times: (a) 0, (b) 0.25, (c) 1, (d) 3, (e) 6, (f) 12, and (g) 24 h.

A structural investigation showed that the crystal transformation occurred from the hexagonal δ-form structure to the triclinic α-form structure during the annealing process. These three patterns showed similar crystal transformation for nylon 11/MMT nanocomposites under annealing. After annealing, the (010,110) reflection representing the intersheet distance became stronger than that of the former pattern because the α-crystalline form became dominant in all nylon 11/MMT cases with an increase in the MMT contents. The annealing treatment increased the reflection intensity of the nanocomposites and made the crystallization and arrangement of hydrogen-bond sheets more perfect. Moreover, these three figures show that the (010,110) reflection was not strong enough, although the annealing time was long enough. This indicated that the hexagonal δ form was reasonably stable.[33]

Figure 7 shows the XRD patterns of nylon 11/MMT nanocomposites annealed at 160°C for 24 h. There is no characteristic peak of MMT basal spacing in Figure 7(a,b). When the MMT concentration was 4 wt %, the characteristic peak of MMT basal spacing was present at 2.3°, corresponding to a basal spacing of 3.46 nm. This observation was consistent with that made from the XRD patterns given in Figure 2. In other words, the morphology of nylon 11/MMT nanocomposites did not change after annealing.

Hydrogen bonds in the nylon 11/MMT nanocomposites

Aliphatic polyamides, such as nylon 6, are well known for their strong hydrogen-bonding ability and seek to maximize the number of hydrogen bonds within and between polymer chains. All possible hydrogen bonds are satisfied in the crystalline regions, and the vast majority is consummated in the amorphous regions.[34] Generally, the addition of silicate layers forces the amide groups of nylon out of the hydrogen-bond sheet and restricts the formation of hydrogen-bond sheets.[30]

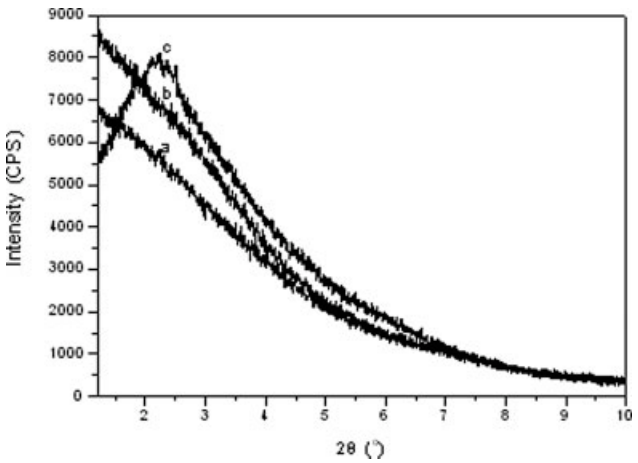

Figure 7 XRD patterns of nylon 11/MMT nanocomposites annealed at 160°C for 24 h with different MMT concentrations: (a) 1, (b) 2, and (c) 4 wt % MMT.

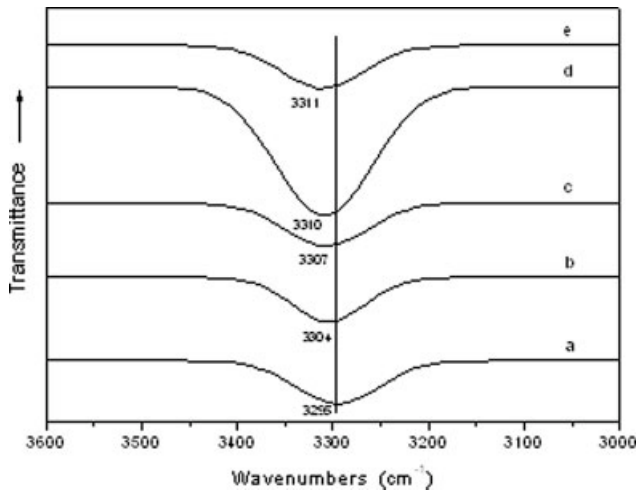

Figure 8 FTIR spectra of nylon 11/MMT nanocomposites with different MMT concentrations: (a) 0, (b) 1, (c) 2, (d) 4, and (e) 6 wt % MMT.

Therefore, the hydrogen bonds of nylon in nylon/MMT nanocomposites will be different from those of neat nylon. Wu and coworkers[35–37] examined the influence of a thermal treatment on the crystallization behavior of nylon 6/clay nanocomposites with FTIR, WAXD, and differential scanning calorimetry and confirmed these conclusions.

The N—H stretching region of nylon ranges from 3100 to 3500 cm^{-1}, and the peak at about 3300 cm^{-1} has been assigned to the hydrogen-bonded N—H stretching mode.[38] Figure 8 shows the IR spectra of nylon 11/MMT nanocomposites with different MMT concentrations at room temperature. For clear observation, we modified the curves with a Gaussian equation. The wave number of the hydrogen-bonded N—H stretching mode shifted to the higher side with increasing MMT contents. This shift trend suggested that the addition of MMT changed the hydrogen bonds of the nanocomposites and weakened the nylon 11 hydrogen bonds, similarly to the nylon 6/MMT nanocomposites.[33] The higher the MMT concentration was, the greater its influence was on the hydrogen bonds.

Figure 9 shows the FTIR spectra of nylon 11/MMT nanocomposites with different MMT concentrations annealed at 160°C for different times. For clear observation, we also modified the curves with a Gaussian equation. It was evident that the N—H stretching band at about 3300 cm^{-1} shifted to the lower wave-number side with increasing annealing time. This change reflected the fact that the hydrogen-bond intensity became higher. During the annealing process, as the lattice of the crystal expanded, the average interchain distance became larger. Therefore, the hydrogen bonds became stronger after annealing, and the nylon 11 crystallized more perfectly with increasing annealing time. This was evidenced by the *d*-spacing of the (100) and (010,110) crystal planes in the nylon 11/MMT nanocomposites with 4 wt % MMT, as shown in Figure 10. It revealed a separate trend for the (100) and (010,110) reflections, in agreement with the FTIR results. It also showed that the pseudohexagonal δ′

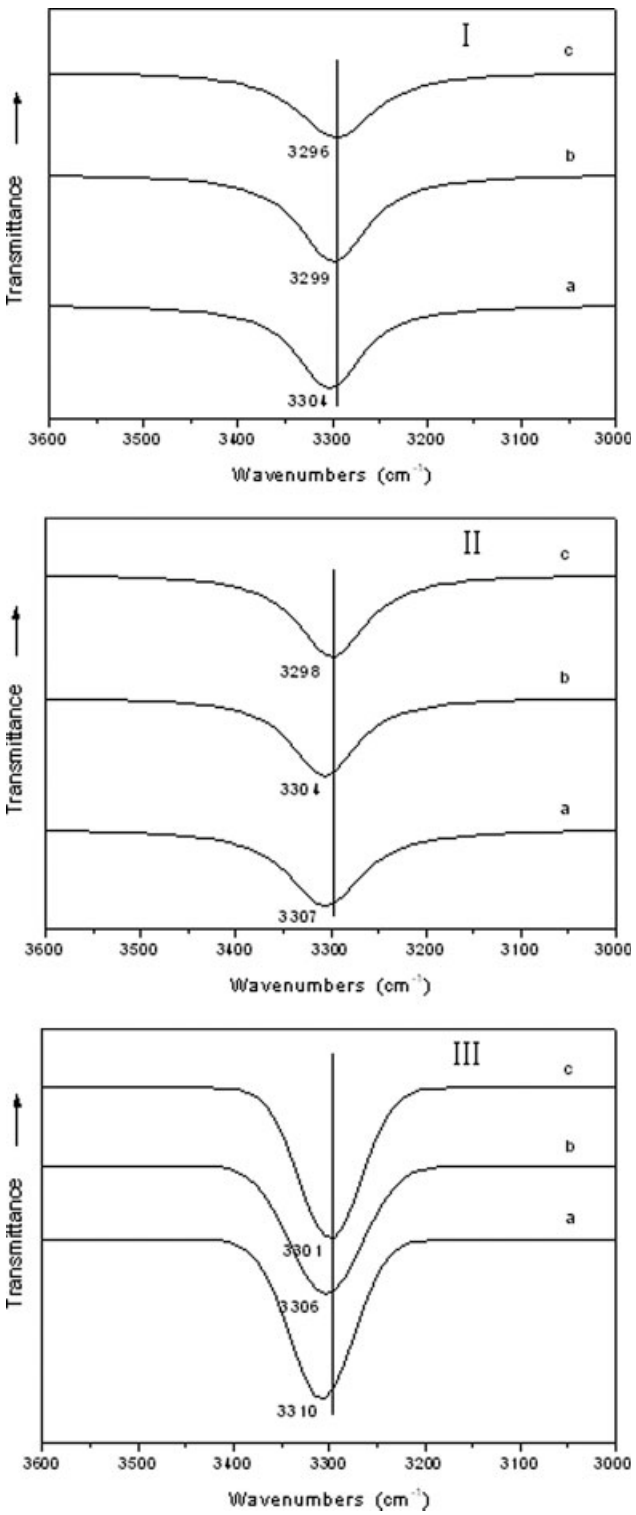

Figure 9 FTIR spectra of nylon 11/MMT nanocomposites with (I) 1, (II) 2, or (III) 4 wt % MMT annealed at 160°C for different times: (a) 0, (b) 3, and (c) 24 h.

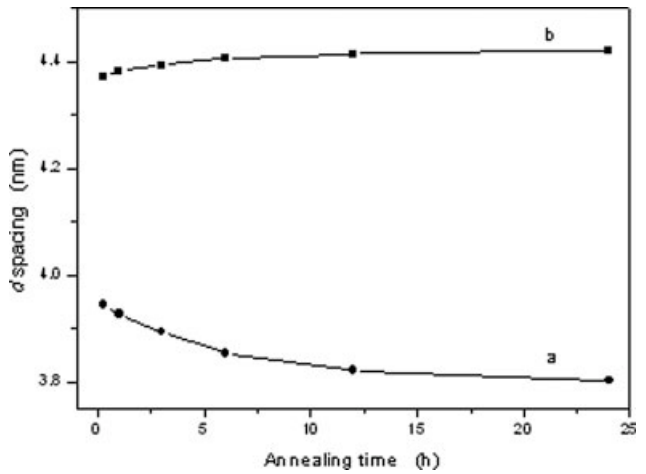

Figure 10 *d*-spacing of a nylon 11/MMT (96/4 wt %) nanocomposite at 160°C for different annealing times: (a) (010,110) reflection plane and (b) (100) reflection plane.

form of nylon 11 tended to transfer to the triclinic α form during the annealing process.[26]

CONCLUSIONS

We prepared exfoliated, layered-silicate-based nylon 11 nanocomposites via *in situ* polymerization. These nylon 11/organoclay nanocomposites were characterized with a number of experimental techniques. XRD and TEM showed that the exfoliated nanocomposites were formed at low clay concentrations (<4 wt %), and a mixture of exfoliated and intercalated nanocomposites was obtained at higher clay concentrations. The nylon 11/MMT nanocomposites displayed polymorphic behavior. The crystal transformation of nylon 11 and nylon 11/MMT nanocomposites under annealing was studied with XRD. The addition of MMT made the crystalline form change from the pseudohexagonal δ′ form to the more stable hexagonal δ form. The results of FTIR demonstrated that the hydrogen bonds of nylon 11 were weakened by the addition of MMT. MMT restricted the formation of hydrogen-bond sheets by forcing the amide groups of nylon out of the hydrogen-bond sheets. The dependence of hydrogen bonds for the nanocomposites on the annealing treatment varied a lot in comparison with neat nylon 11, especially when the annealing time was prolonged.

References

1. Messersmith, P. B.; Stupp, S. I. J Mater Res 1992, 7, 2559.
2. Komarneni, S. J Mater Chem 1992, 2, 1219.
3. Giannelis, E. P. Adv Mater 1996, 8, 29.
4. Usuki, A.; Kojima, Y.; Kawasumi, M.; Okada, A.; Fukushima, Y.; Kurauchi, T.; Kamigaito, O. J Mater Res 1993, 8, 1179.
5. Usuki, A.; Kojima, Y.; Kawasumi, M. J Polym Sci Part A: Polym Chem 1993, 31, 1175.
6. Kojima, Y.; Usuki, A.; Kawasumi, M.; Okada, A.; Kurauchi, T.; Kamigaito, O. J Polym Sci Part A: Polym Chem 1993, 31, 983.
7. Kojima, Y.; Usuki, A.; Kawasumi, M.; Okada, A.; Fukushima, Y.; Kurauchi, T.; Kamigaito, O. J Mater Res 1993, 8, 1185.
8. Kojima, Y.; Matsuoka, T.; Takahashi, H.; Kurauchi, T. J Appl Polym Sci 1994, 51, 683.
9. Mathias, L. J.; Davis, R. D.; Jarrett, W. L. Macromolecules 1999, 32, 7958.
10. Liu, L.; Qi, Z.; Zhu, X. J Appl Polym Sci 1999, 71, 1133.
11. Jimenez, G.; Ogata, N.; Kawai, H.; Ogihara, T. J Appl Polym Sci 1997, 64, 2211.
12. Fornes, T. D.; Yoon, P. J.; Keskkula, H.; Paul, D. R. Polymer 2001, 42, 9929.
13. Fornes, T. D.; Yoon, P. J.; Keskkula, H.; Paul, D. R. Polymer 2002, 43, 2121.
14. Wu, T. M.; Blackwell, J. Macromolecules 1996, 29, 5621.
15. Wu, T. M.; Blackwell, J. J Polym Res 1997, 4, 25.
16. Gurato, G.; Fichera, A.; Grandi, F. Z.; Zannetti, R.; Canal, P. Macromol Chem 1974, 175, 953.
17. Gogolewski, S.; Gasiorek, M.; Czerniawska, K.; Pennings, A. J. Colloid Polym Sci 1982, 260, 859.
18. Liu, X. H.; Wu, Q. J.; Berglund, L. A. Polymer 2002, 43, 4967.
19. Slichter, W. P. J Polym Sci 1959, 36, 259.
20. Newman, B. A.; Sham, T. P.; Pae, K. D. J Appl Phys 1977, 48, 4092.
21. Kawaguchi, A.; Ikawa, T.; Fujiwara, Y.; Tabuchi, M.; Konobe, K. J Macromol Sci Phys 1981, 20, 1.
22. Kim, K. G.; Newman, B. A.; Scheinbeim, J. I. J Polym Sci Polym Phys Ed 1985, 23, 2477.
23. Kinoshita, Y. Macromol Chem 1959, 33, 1.
24. Sasaki, T. J Polym Sci Part B: Polym Lett 1965, 3, 557.
25. Yu, H. H. Mater Chem Phys 1998, 56, 289.
26. Zhang, Q. X.; Mo, Z. S.; Zhang, H. F.; Liu, S. Y.; Cheng, S. Z. D. Polymer 2001, 42, 5543.
27. Zhang, G. S.; Li, Y. J.; Yan, D. Y. J Polym Sci Part B: Polym Phys 2004, 42, 253.
28. Zhang, Q.; Yu, M.; Fu, Q. Polym Int 2004, 53, 1941.
29. Lee, J. W.; Takase, Y.; Newman, B. A.; Scheinbeim, J. I. J Polym Sci Part B: Polym Phys 1991, 29, 273.
30. Lincoln, D. M.; Vaia, R. A.; Wang, Z. G.; Hsiao, B. S. Polymer 2001, 42, 1621.
31. Statton, W. O. J Polym Sci Part C: Polym Symp 1967, 18, 33.
32. Murthy, N. S.; Curran, S. A.; Aharoni, S. M.; Minor, H. Macromolecules 1991, 24, 3215.
33. Balizer, E.; Fedderly, J.; Haught, D.; Dickens, B.; Dereggi, A. S. J Polym Sci Part B: Polym Phys 1994, 32, 365.
34. Aharoni, S. M. n-Nylons: Their Synthesis, Structure, and Properties; Wiley: Chichester, England, 1997.
35. Wu, Q.; Liu, X.; Berglund, L. A. Polymer 2002, 43, 2445.
36. Wu, Q.; Liu, X.; Berglund, L. A. Macromol Rapid Commun 2001, 22, 1438.
37. Liu, X.; Wu, Q. Polymer 2002, 43, 1933.
38. Skrovanek, D.; Howe, S. E.; Painter, P. C.; Coleman, M. M. Macromolecules 1986, 19, 699.